Corticotropin releasing hormone receptor 2 exacerbates chronic cardiac dysfunction

Takuma Tsuda,[1]* Mikito Takefuji,[1]* Nina Wettschureck,[2] Kazuhiko Kotani,[3] Ryota Morimoto,[1] Takahiro Okumura,[1] Harmandeep Kaur,[2] Shunsuke Eguchi,[1] Teruhiro Sakaguchi,[1] Sohta Ishihama,[1] Ryosuke Kikuchi,[4] Kazumasa Unno,[1] Kunihiro Matsushita,[5] Shizukiyo Ishikawa,[3] Stefan Offermanns,[2] and Toyoaki Murohara[1]

[1]Department of Cardiology, Nagoya University School of Medicine, Nagoya, Japan
[2]Department of Pharmacology, Max Planck Institute for Heart and Lung Research, Bad Nauheim, Germany
[3]Center for Community Medicine, Jichi Medical University, Shimotsuke, Japan
[4]Department of Medical Technique, Nagoya University Hospital, Nagoya, Japan
[5]Department of Epidemiology, Johns Hopkins Bloomberg School of Public Health, Baltimore, MD

Heart failure occurs when the heart is unable to effectively pump blood and maintain tissue perfusion. Despite numerous therapeutic advancements over previous decades, the prognosis of patients with chronic heart failure remains poor, emphasizing the need to identify additional pathophysiological factors. Here, we show that corticotropin releasing hormone receptor 2 (Crhr2) is a G protein–coupled receptor highly expressed in cardiomyocytes and continuous infusion of the Crhr2 agonist, urocortin 2 (Ucn2), reduced left ventricular ejection fraction in mice. Moreover, plasma Ucn2 levels were 7.5-fold higher in patients with heart failure compared to those in healthy controls. Additionally, cardiomyocyte-specific deletion of Crhr2 protected mice from pressure overload–induced cardiac dysfunction. Mice treated with a Crhr2 antagonist lost maladaptive 3′-5′-cyclic adenosine monophosphate (cAMP)–dependent signaling and did not develop heart failure in response to overload. Collectively, our results indicate that constitutive Crhr2 activation causes cardiac dysfunction and suggests that Crhr2 blockade is a promising therapeutic strategy for patients with chronic heart failure.

INTRODUCTION

Heart failure is a common cardiovascular disease with poor prognosis that develops when the heart is unable to pump blood and maintain tissue perfusion (Fang et al., 2008; Yancy et al., 2013). Despite improvements in the treatment of cardiovascular diseases, such as coronary heart disease and hypertension, the prognosis of heart failure remains poor (Braunwald, 2013). Several mechanisms contribute to the development of heart failure following valve disease, cardiomyopathy, or after myocardial infarction (Frey and Olson, 2003; Jessup and Brozena, 2003; Heineke and Molkentin, 2006). In most cases, cardiac remodeling occurs in response to environmental demands, and various stimuli, such as hormonal activation and hypertension, inducing cardiac hypertrophy. Hypertrophic growth is the primary mechanism to reduce stress on the ventricular wall; however, the heart undergoes irreversible decompensation with prolonged stress, resulting in heart failure (Hill and Olson, 2008).

All cells possess transmembrane signaling systems responsive to extracellular stimuli. G protein–coupled receptors (GPCRs) are the largest superfamily of cell surface receptors and are involved in numerous physiological and pathological processes (Katritch et al., 2013). GPCR-mediated signaling is implicated in various diseases, including metabolic, immunological, and neurodegenerative disorders, as well as cancer and infection (Heng et al., 2013); thus, GPCRs are considered to be attractive drug targets (Overington et al., 2006).

In the heart, GPCRs regulate cardiac function in response to extracellular stimuli, such as catecholamines and angiotensin II, and play a role in cardiac dysfunction and fibrosis (Wettschureck and Offermanns, 2005). GPCR inhibitors are widely used to treat patients with heart failure (Kang et al., 2007; Capote et al., 2015). Although the heart expresses several GPCRs (Regard et al., 2008), only β adrenergic and angiotensin II receptors antagonists are clinically used as a long-term treatment for patients with chronic heart failure. Despite these available therapies, mortality and hospitalization rates have remained relatively high for over a decade, suggest-

*T. Tsuda and M. Takefuji contributed equally to this paper.

Correspondence to Mikito Takefuji: takefuji@med.nagoya-u.ac.jp

Abbreviations used: BMI, body mass index; BNP, brain natriuretic peptide; cAMP, 3′-5′-cyclic adenosine monophosphate; CREB, cAMP response element binding protein; Crh, corticotropin releasing hormone; Crhr2, Crh receptor 2; EPAC, exchange protein directly activated by cAMP; GPCR, G protein–coupled receptor; NIDCM, nonischemic dilated cardiomyopathy; PI3K, phosphatidylinositol 3-kinase; PKA, cAMP-dependent protein kinase; qRT-PCR, quantitative RT-PCR; Ryr2, ryanodine receptor 2; SBP, systolic blood pressure; TAC, transverse aortic constriction; Ucn2, urocortin 2.

The Rockefeller University Press $30.00
J. Exp. Med. 2017
https://doi.org/10.1084/jem.20161924

The Journal of Experimental Medicine

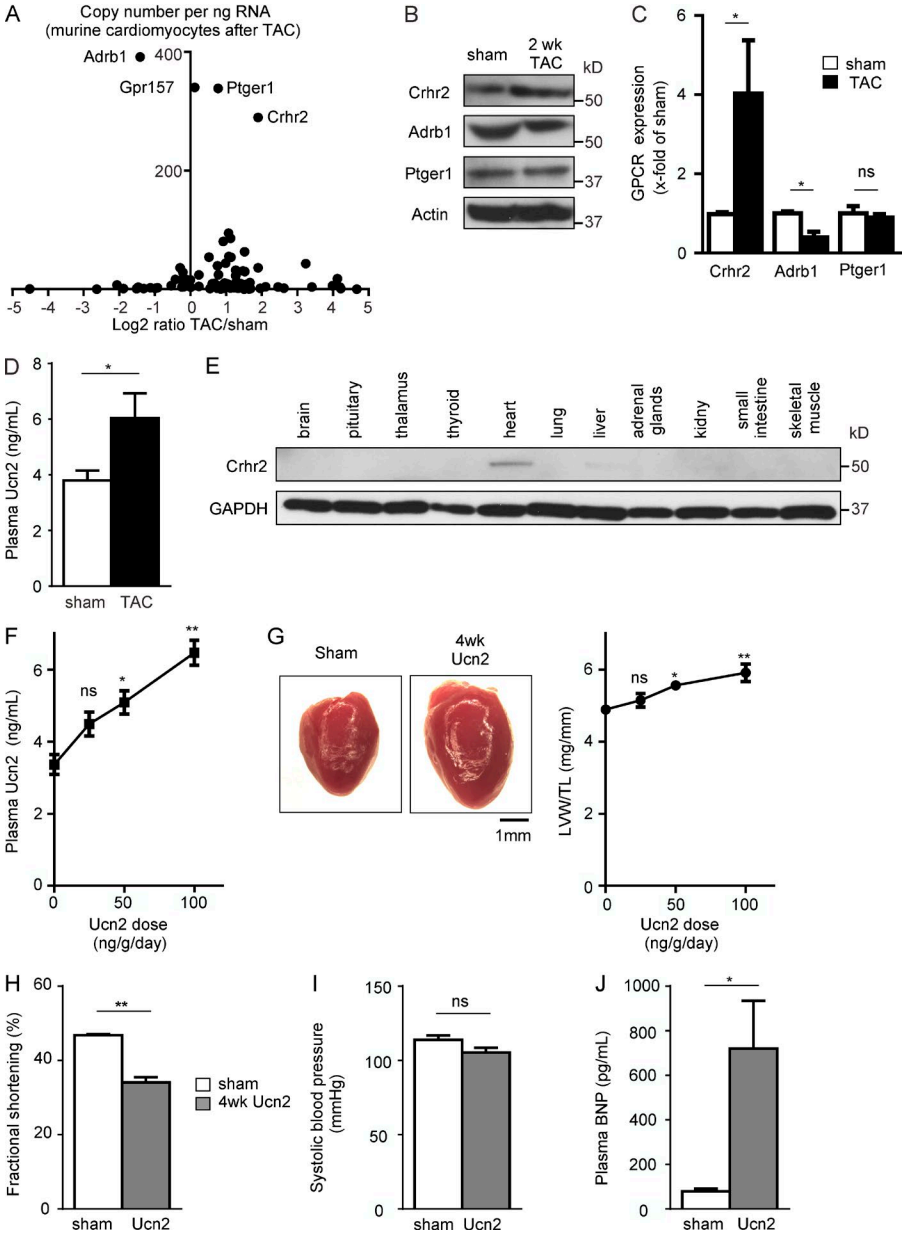

Figure 1. **Sustained Crhr2 activation induces cardiac dysfunction.** (A) G-protein–coupled receptor (GPCR) gene expression analysis in isolated cardiomyocytes 2 wk after transverse aortic constriction (TAC) using qRT-PCR greater than five copies per ng of RNA. The results are representative of two independent experiments. (B) Protein expression of Crhr2, adrenoceptor β-1 receptor (Adrb1), and prostaglandin E receptor 1 (Ptger1) in left ventricles 2 wk after sham or TAC was determined by immunoblotting analysis. (C) Statistical evaluation of (B; sham set to 1; $n = 3$; two-tailed Student's t test). (D) Plasma Ucn2 concentration 2 wk after sham or TAC (n = 17; two-tailed Student's t test). (E) Crhr2 tissue distribution in humans. (F and G) Plasma Ucn2 concentration (F), and cardiac morphology, left ventricular weight/tibia length (LVW/TL) ratio (G) after 4 wk of sustained Ucn2 infusion ($n = 5$; two-way ANOVA and Bonferroni post-hoc test). (H) Left ventricular fractional shortening determined by echocardiogram after 4 wk of sustained Ucn2 infusion ($n = 5$; two-tailed Student's t test). (I) Systolic blood pressure after 4 wk of sustained Ucn2 infusion ($n = 5$; two-tailed Student's t test). (J) Plasma BNP concentration after 4 wk of sustained Ucn2 infusion (n = 5, 2-tailed Student's t test). Error bars indicate SEM. *, $P < 0.05$; **, $P < 0.01$; ns, not significant. The results are representative of three independent experiments (B–J).

ing that additional uncharacterized factors may also mediate disease pathophysiology (Tamargo and López-Sendón, 2011).

Here, we report that the GPCR corticotropin releasing hormone receptor 2 (Crhr2) is highly expressed in the heart and facilitates heart failure. Notably, constitutive Crhr2 activation incites cardiac dysfunction in mice and serum levels of the Crhr2 agonist urocortin2 (Ucn2) were markedly higher in patients with heart failure than in healthy controls. Moreover, Crhr2 antagonist treatment mitigated pressure overload-induced cardiac dysfunction in mice and suppressed maladaptive gene expression mediated by 3′-5′-cyclic adenosine monophosphate (cAMP) response element binding protein (CREB), as well as pathological cardiac dysfunction induced by exchange protein directly activated by cAMP (EPAC)/CaMKII signaling. Thus, our results indicate that Crhr2 may be a promising therapeutic target for chronic heart failure.

RESULTS AND DISCUSSION

Continuous Crhr2 activation causes heart failure in mice

A systematical search was performed to identify GPCRs expressed in cardiomyocytes and related to heart failure. For this, we performed non-biased quantitative RT-PCR (qRT-PCR) analysis to determine the gene copy number of 475 GPCRs in adult murine cardiomyocytes 2 wk after sham procedure or transverse aortic constriction (TAC; Fig. S1). Data revealed that adult murine cardiomyocytes expressed about 80 GPCRs (>5 copies per ng of RNA), the most abundant

Table 1. **Comparison of each parameter between controls and patients with NIDCM**

Parameters	Control	HF (NIDCM)	P-value
	n = 260	*n* = 52	
Age, yr	57.6 ± 10.5	57.4 ± 10.7	0.94
Gender, male (%)	140 (54%)	28 (54%)	1
BMI, kg/m2	22.3 ± 2.9	22.7 ± 4.3	0.51
SBP, mmHg	133 ± 18	119 ± 20	<0.01[a]
DBP, mmHg	80 ± 11	73 ± 13	<0.01[a]
Total Cholesterol, mg/dl	203 ± 34	195 ± 37	0.13
Glucose, mg/dl	96 ± 10	99 ± 24	0.27
Creatinine, mg/dl	0.73 ± 0.15	0.86 ± 0.22	<0.01[a]
Ucn2, pg/ml	235 (54–647)	1,755 (1,166–3,130)	<0.01[a]

HF, heart failure; DBP, diastolic blood pressure. Data represent means ± SD, medians (interquartile ranges), or subject numbers (%).
[a]P < 0.01 (unpaired Student's *t* test or Chi-square test).

being *Crhr2*, *Adrb1*, *Ptger1*, and *Gpr157* (Fig. 1 A). Crhr2 expression was markedly increased at the gene and protein level in the left ventricle 2 wk after TAC, whereas that of Adrb1 was decreased and Ptger1 expression was unchanged (Fig. 1, B and C). Moreover, TAC significantly increased Ucn2 levels in the blood (Fig. 1 D). Western blot analysis of various human tissues indicated that Crhr2 is exclusively expressed in the heart and is undetectable in other tissues (Fig. 1 E). Together, these results indicate that Crhr2 is highly expressed in cardiomyocytes and increases after pressure overload–induced heart failure.

Acute intravenous injection of Ucn2 has been shown to accelerate cardiac contraction (Coste et al., 2000), but whether a chronic increase in plasma Ucn2 levels affects cardiac function remains unknown. To examine the effect of long-term Ucn2 up-regulation in vivo, we implanted mice with osmotic pumps that release Ucn2. After 4 wk of sustained Ucn2 infusion, blood analysis revealed that circulating Ucn2 levels were elevated similar to those observed after TAC (Fig. 1 F). In addition, animals showed cardiac hypertrophy with an increased left ventricular weight to tibia length ratio in a dose-dependent manner (Fig. 1 G), which was accompanied by a decrease in left ventricular fractional shortening (Fig. 1 H) without significantly affecting systolic blood pressure (SBP; Fig. 1 I). Moreover, continuous Ucn2 infusion significantly increased blood levels of brain natriuretic peptide (BNP), which is secreted by cardiomyocytes in response to pressure and volume overload (Fig. 1 J; Doust et al., 2005). Collectively, these results indicate that chronic increase in plasma Ucn2 impairs cardiac function.

Increased plasma Ucn2 levels in patients with heart failure

Based on these findings, we measured plasma Ucn2 levels in 260 healthy subjects (plasma BNP < 5.8 pg/ml) and 52 patients with non-ischemic dilated cardiomyopathy (NIDCM; plasma BNP = 246.8 ± 362 pg/ml). The clinical demographics of the patient population are shown in Table 1. Although both groups presented with similar body mass index (BMI), plasma total cholesterol, and plasma glucose levels, patients with NIDCM showed significantly lower SBP and diastolic blood pressure, as well as significantly higher creatinine levels. Of note, patients with NIDCM exhibited significantly higher Ucn2 levels (a median 7.5-fold increase) than healthy controls, which remained significant after adjustment for all measured parameters ($P < 0.01$). Thus, these data indicate that increased plasma Ucn2 is strongly associated with heart failure in humans, suggesting that Ucn2 measurement may be a novel diagnostic marker for chronic heart failure.

Attenuated cardiac hypertrophy, fibrosis, and heart failure in Crhr2-deficient mice

To examine the functional significance of Crhr2 in cardiomyocytes in vivo, we generated mice with tamoxifen-inducible cardiomyocyte-specific Crhr2 deficiency (cmc-Crhr2 KO) by mating αMHC-Cre-ERT2 mice with $Crhr2^{flox/flox}$ animals. The efficiency of tamoxifen-inducible recombination was analyzed by Western blotting, which showed that Crhr2 was undetectable in cardiomyocytes isolated from tamoxifen-treated cmc-Crhr2 KO mice (Fig. 2 A). No differences were observed in the ratio of left ventricular weight to tibia length or cardiac function before and after tamoxifen treatment in cmc-Crhr2 KO mice (Fig. 2, B and C). Notably, cmc-Crhr2 KO mice failed to show a Ucn2-induced hypertrophic response (Fig. 2 B). In addition, although 4 wk of continuous Ucn2 infusion decreased fractional shortening in control mice, this was significantly attenuated in cmc-Crhr2-KO mice (Fig. 2 C). These results indicate that continuous Ucn2 infusion directly affects cardiomyocytes via Crhr2.

To investigate whether cardiomyocyte-specific Crhr2 deficiency protected mice from pressure overload-induced cardiac dysfunction, we performed TAC surgeries in cmc-Crhr2 KO mice. In control mice, TAC resulted in a significant increase in cardiac hypertrophy as determined by postmortem analysis of the ratio of left ventricular weight to tibia length, whereas cmc-specific Crhr2 KO mice showed a significantly lower ratio of left ventricular weight to tibia length (Fig. 2 D). We also found that cmc-specific Crhr2 KO mice showed significantly less fi-

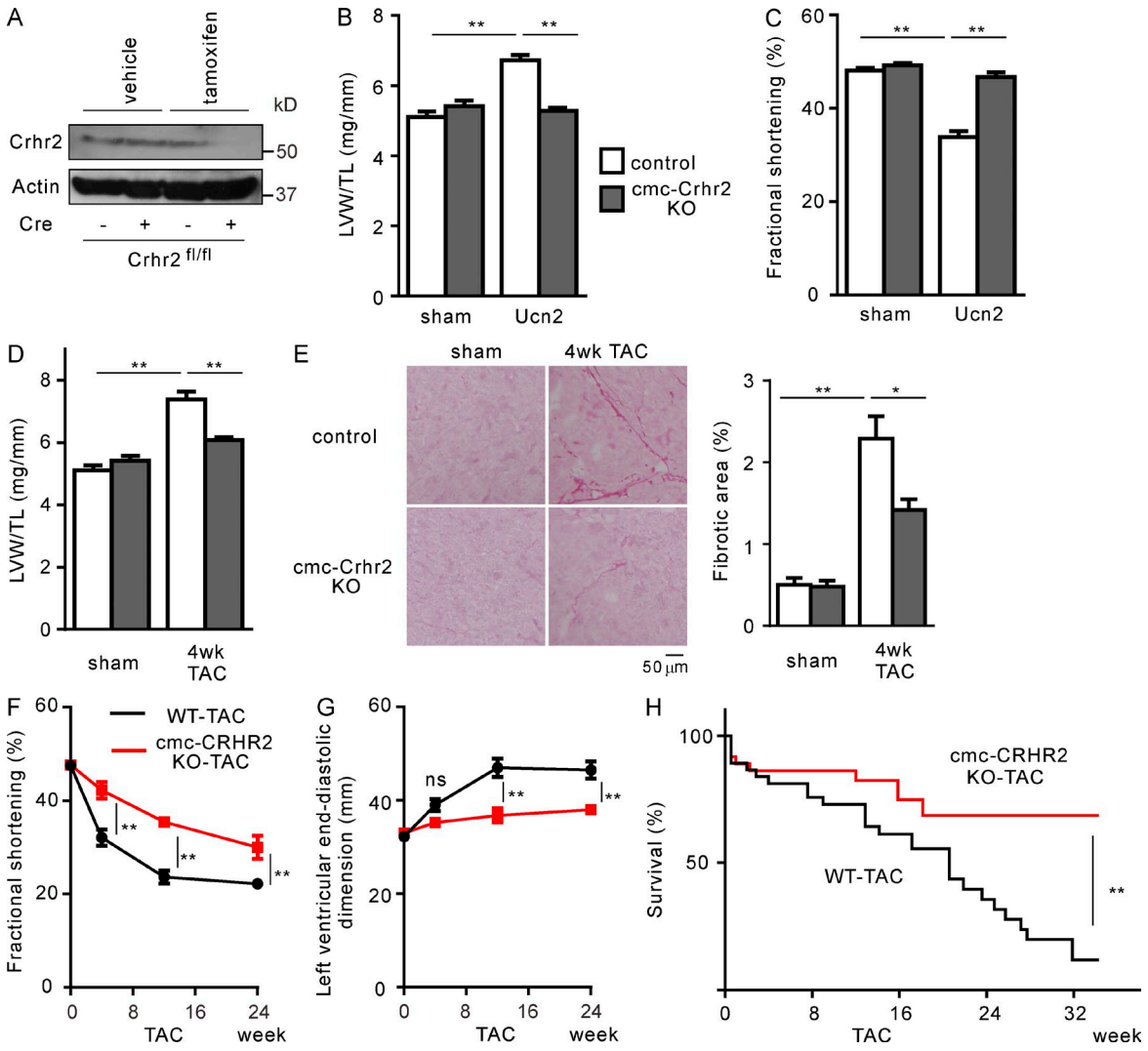

Figure 2. **Cardiomyocyte-specific, Crhr2-deficient mice exhibit suppressed pressure overload–induced cardiac dysfunction.** (A) Protein extracts from isolated cardiomyocytes of vehicle- or tamoxifen-treated α-myosin heavy chain (αMHC)-CreERT2 (Cre)-negative and -positive Crhr2$^{flox/flox}$ mice were blotted with antibodies against Crhr2 and actin. (B and C) LVW/TL ratio (B) and left ventricular fractional shortening (C) 4 wk after continuous infusion of Ucn2 or vehicle (sham) through an osmotic pump (n = 6; two-way ANOVA and Bonferroni post-hoc test). (D) LVW/TL ratio 4 wk after transverse aortic constriction (TAC; n = 6–10; two-way ANOVA and Bonferroni post-hoc test). (E) Fibrotic changes in left ventricles 4 wk after TAC were assessed by PicroSirius red staining (n = 4; two-way ANOVA and Bonferroni post-hoc test). (F and G) Left ventricular fractional shortening (F) and left ventricular end-diastolic dimension (G) were assessed by echocardiogram before and 4, 12, and 24 wk after TAC (n = 6; two-way ANOVA and Bonferroni post-hoc test). (H) Survival plot for control mice and cmc-Crhr2-KOs up to 8 mo after TAC (n = 36–37; Log-rank test). Error bars indicate SEM. *, P < 0.05; **, P < 0.01; ns, not significant. The results are representative of three independent experiments (A–G).

brosis 4 wk after TAC as determined by PicroSirius red staining (Fig. 2 E). Furthermore, cmc-Crhr2 KO mice were resistant to further deterioration of the left ventricular fractional shortening as determined by echocardiography at 4, 12, and 24 wk after TAC (Fig. 2 F). Ventricular dilation was also observed 12 wk after TAC in wild-type mice, but not in cmc-Crhr2 KO mice (Fig. 2 G). Crhr2 deficiency significantly improved mortality 8 mo after TAC (Fig. 2 H). Collectively, these results demonstrate that cardiomyocyte-specific Crhr2-deficient mice are resistant to pressure overload-induced cardiac dysfunction.

Effect of Crhr2 antagonist on pressure overload-induced cardiac dysfunction

We next investigated whether treatment with the Crhr2 antagonist, antisauvagine-30 (Rühmann et al., 1998), would attenuate the progression of established cardiac hypertrophy in mice. For this, continuous antisauvagine-30 infusion was initiated 1 wk after TAC surgery (Fig. 3 A). Interestingly, Crhr2 antagonist treatment protected mice from further deterioration of cardiac output without significantly affecting SBP (Fig. 3, B and C). These protective effects were accompanied by a strong reduction of plasma BNP, cardiac hypertrophy,

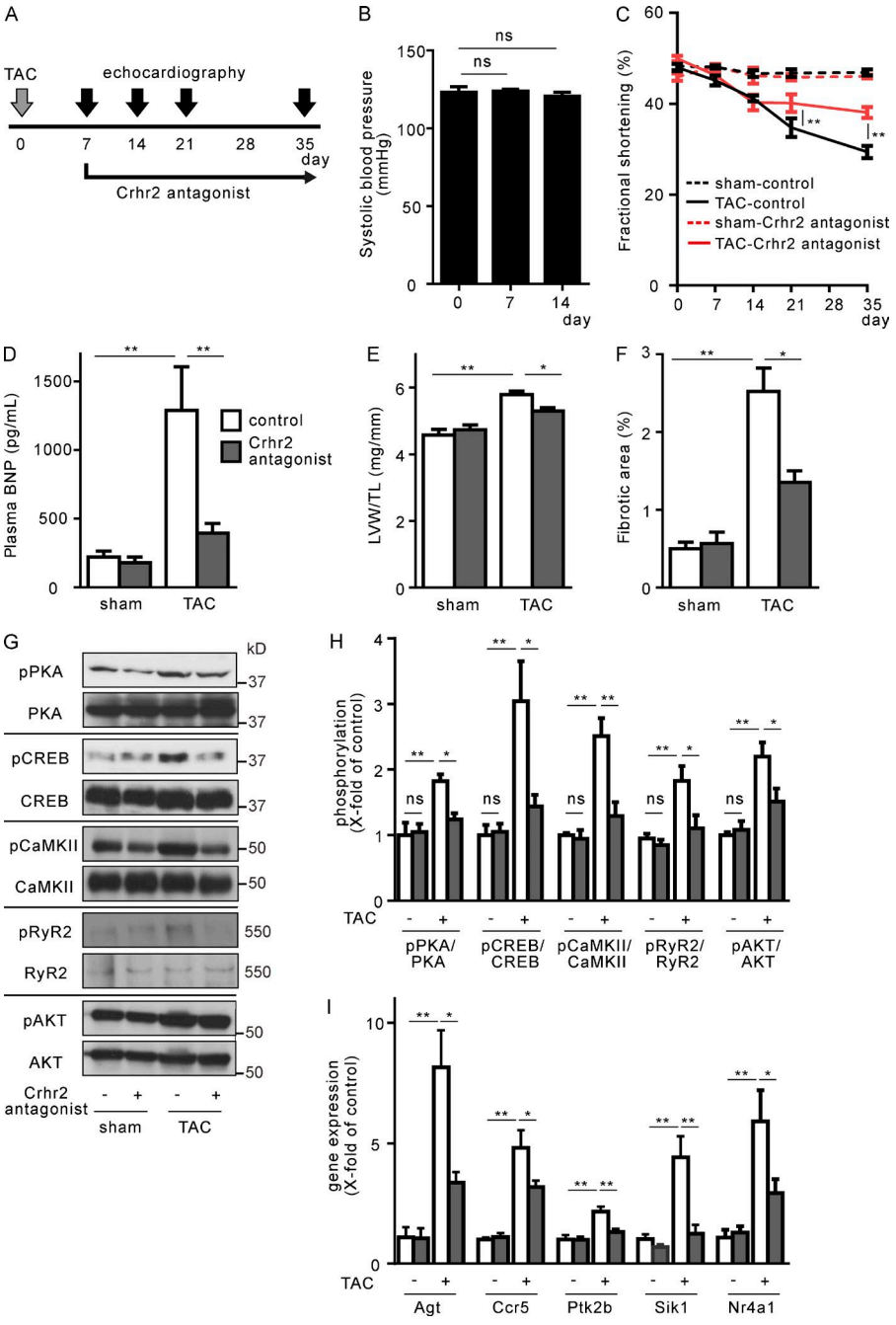

Figure 3. **Crhr2 antagonist treatment suppressed pressure overload–induced cardiac dysfunction in preexisting hypertrophy.** (A) Experimental design. (B) Systolic blood pressure in sham mice with Crhr2 antagonist treatment (n = 5; two-way ANOVA and Bonferroni post-hoc test). (C) Echocardiogram analysis of left ventricular fractional shortening was performed before and 7, 14, 21, and 35 d after TAC surgery (n = 5; two-way ANOVA and Bonferroni post-hoc test). (D–F) Plasma BNP (D), LVW/TL (E), and fibrotic area (determined by Picro-Sirius red staining; F) were measured 35 d after TAC surgery (n = 8–10; two-way ANOVA and Bonferroni post-hoc test). (G and H) Immunoblotting showed PKA, CREB, CaMKII, RyR2, and AKT phosphorylation in response to TAC in the heart with or without Crhr2 antagonist treatment (n = 4; two-way ANOVA and Bonferroni post-hoc test). (I) Gene expression 4 wk after Crhr2 antagonist treatment as determined by qRT-PCR in whole hearts (n = 4–6; two-way ANOVA and Bonferroni post-hoc test). Error bars indicate SEM. *, $P < 0.05$; **, $P < 0.01$; ns, not significant. The results are representative of two independent experiments (B–I).

and cardiac fibrosis (Fig. 3, D–F). Conversely, 4 wk of Ucn2 infusion accelerated TAC-induced cardiac dysfunction (Fig. S2, A–E). These results suggest that Crhr2 blockade may be a novel therapeutic approach to treat chronic heart failure.

Therapeutic mechanism of Crhr2 antagonist during heart failure

Most GPCRs are coupled to heterotrimeric G-proteins, resulting in the activation of respective cellular signaling pathways (Wettschureck and Offermanns, 2005; Salazar et al., 2007). Crhr2 activation increases intracellular cAMP levels, strongly suggesting that Crhr2 is coupled to the G-protein, Gαs (Kishimoto et al., 1995; Stenzel et al., 1995). To study Crhr2-mediated G-protein signaling, we measured the activation of individual G-protein–mediated response elements by luciferase reporter assays, which confirmed that Crhr2 induced Gαs-mediated signaling, but not that of Gαq, Gαi, or Gα12 (Fig. S3, A and B). In addition, chronic increases in intracellular cAMP are associated with cardiotoxicity during heart failure (Boularan and Gales, 2015). Currently, β adrenergic stimulation is believed to be primarily responsible for the uncontrolled cellular cAMP accumulation observed during

cardiac hypertrophy and heart failure (Engelhardt et al., 1999; Lymperopoulos et al., 2013).

Because Ucn2 acts via several signaling pathways, including cAMP-dependent protein kinase A (PKA), EPAC, and phosphatidylinositol 3-kinase (PI3K)/AKT (Adão et al., 2015), we further investigated whether Crhr2 inactivation could reduce the elevated cAMP signaling found during heart failure by examining the phosphorylation cascade of PKA (Steinberg et al., 1993), which undergoes activating phosphorylation at Thr197, and CREB, which binds CRE and stimulates transcription after PKA-mediated Ser133 phosphorylation (Mayr and Montminy, 2001; Altarejos and Montminy, 2011). We also investigated other mechanistic pathways. For example, EPAC/CaMKII signaling can regulate cAMP-dependent cardiovascular functions in a PKA-independent manner to enhance vascular endothelial barrier stability and vasorelaxation, although chronic EPAC activation in the heart causes arrhythmia and heart failure (Lezoualc'h et al., 2016). Moreover, EPAC elicits CaMKII Thr286/287 autophosphorylation, downstream ryanodine receptor 2 (RyR2) Ser2814 phosphorylation, and Ca^{2+} release from the sarcoplasmic reticulum, which subsequently contributes to arrhythmias and pathological cardiac hypertrophy (Anderson et al., 2011). In addition, EPAC/CaMKII can also regulate histone deacetylases (HDACs) to induce myocyte enhancer factor 2 (MEF2)–mediated hypertrophic gene expression.

Alternatively, PI3Ks, which are intracellular lipid kinases regulated by the growth factor receptor tyrosine kinase and by GPCR-mediated Gβγ subunit binding (Engelman et al., 2006), may be involved in our observed Ucn2 effects. We examined PI3K-mediated AKT Ser473 phosphorylation, which contributes to both physiological and pathological cardiac hypertrophy. We found that Ucn2 stimulation enhanced PKA, CREB, CaMKII, RyR2, and AKT phosphorylation in isolated murine cardiomyocytes and in the heart (Fig. S3, C–E). Moreover, Crhr2 antagonist treatment markedly decreased TAC-induced PKA, CREB, CaMKII, RyR2, and AKT phosphorylation in the heart (Fig. 3, G and H), indicating that Crhr2 antagonism suppressed TAC-induced Gαs/PKA/CREB/CRE, Gαs/EPAC/CaMKII/RyR2, and Gβγ/AKT pathway activity. To identify Crhr2-regulated genes, we performed whole-genome expression profiling in hearts from mice subjected to continuous infusion of Ucn2 or vehicle for 2 wk. Notably, 88 genes were >1.5-fold up-regulated in wild-type mice in response to Ucn2, of which seven (*Agt*, *Ccr5*, *Foxo3*, *Irs2*, *Ptk2b*, *Sik1*, and *Nr4a1*) overlapped between predicted CREB- or MEF2-mediated genes and heart failure–related genes (Fig. S3 F; Jhala et al., 2003; Backs and Olson, 2006; Berdeaux et al., 2007; Banerjee et al., 2011; Shimizu et al., 2013). Subsequent analysis showed that Crhr2 antagonist infusion significantly suppressed the TAC-induced expression of *Agt*, *Ccr5*, *Ptk2b*, *Sik1*, and *Nr4a1* (Fig. 3 I), indicating that Crhr2 blockade suppressed maladaptive CREB- and MEF2-mediated gene expression in the heart, thereby preventing cardiac dysfunction.

Data from the present study shows that Crhr2 is abundantly expressed in cardiomyocytes and its expression increases in pressure overload–induced cardiac dysfunction. There are two Crhr isoforms, termed Crhr1 and Crhr2 (Bale and Vale, 2004). Crhr1 is mainly expressed in the brain and pituitary gland, whereas Crhr2 mRNA expression in mice is found in peripheral tissues, such as the heart, liver, and skeletal muscle (Kishimoto et al., 1995; Stenzel et al., 1995; Chen et al., 2005). Moreover, Crhr1 appears to be responsible for stimulating the release of adrenocorticotrophic hormone in stress responsivity; however, the role of endogenous Crhr2 remains unclear. Our study demonstrated that Crhr2 protein is abundantly expressed in the human heart, and plasma Ucn2 levels were higher in patients with heart failure compared to healthy controls, indicating that endogenous Crhr2 is associated with heart failure in humans. Our findings are supported by clinical trials in heart failure that reported increased plasma Ucn2 was associated with heart failure (Davis et al., 2007a,b; Adão et al., 2015).

The Crh peptide family activates the PKA, CaMKII, and AKT signaling pathways to temporarily increase cardiac function (Adão et al., 2015), but the effects of chronic activation of these pathways in the heart remains controversial. Preclinical studies showed that acute Crhr2 agonist infusion increases cardiac output by decreasing SBP (Chan et al., 2013). Similarly, adenovirus-mediated Ucn2 overexpression in the liver (>15-fold) increased cardiac output in mice (Gao et al., 2013). However, the physiological effects of prolonged increases in plasma Ucn2 levels and Crhr2 antagonist therapy have not been investigated in heart failure. Our data demonstrated that continuous Crhr2 agonist infusion increased plasma Ucn2 two-fold similar to that observed after TAC without a significant effect on blood pressure and resulted in cardiac dysfunction, whereas its blockade suppressed pressure overload-induced chronic cardiac dysfunction. These findings suggest that chronic Ucn2 activation without vasorelaxation may have cardiotoxic effects.

Because estrogen increases Ucn2 levels and Crhr2 expression in cardiomyocytes (Cong et al., 2014), another consideration is whether there are gender differences in the role of Ucn2 in the heart. We implanted female mice with osmotic pumps that release Ucn2 and found that 4 wk of Ucn2 infusion caused a significantly increased left ventricular weight to tibia length and decreased ventricular fractional shortening (unpublished data). Additionally, cmc-Crhr2 KO female mice were resistant to TAC-induced cardiac hypertrophy and Crhr2 antagonist treatment protected female mice from further TAC-induced cardiac dysfunction similar to that observed in male mice (personal correspondence). These findings indicate that there are no gender differences in the role of Crhr2 in heart failure.

Based on our findings, although acute Ucn2 injection has been shown to increase cardiac function, chronic elevations in Ucn2 are associated with cardiac dysfunction. These opposing effects may be similar to that found with cardiac

β adrenergic receptors, which are also coupled to Gαs. Although adrenaline treatment is beneficial during the acute phase, β blockers have become a frontline drug for the treatment of chronic heart failure (Braunwald, 2001). It is known that cellular signaling is adaptive in acute heart failure, and can cause maladaptive cardiac remodeling over prolonged periods of time. Most GPCRs are coupled to more than one heterotrimeric G-protein, resulting in activation of specific intracellular pathways. Cardiac Gαs transgenic mice exhibit progressive cardiac dysfunction with cardiac apoptosis, cardiac hypertrophy, and cardiac fibrosis as the mice age (Iwase et al., 1996; Geng et al., 1999). Cardiac PKA transgenic mice display ventricular dilation and decreased cardiac function (Antos et al., 2001), and PKA phosphorylation is significantly elevated in failing hearts from humans and animal models (Marx et al., 2000). Similarly, CREB phosphorylation promotes target gene expression (Mayr and Montminy, 2001; Altarejos and Montminy, 2011), although the functional significance of CREB in the normal heart is controversial. For instance, cardiac-specific overexpression of dominant-negative CREB induced cardiac dysfunction (Fentzke et al., 1998); however, CREB-deficient mice display no changes in cardiac morphology (Matus et al., 2007). Nevertheless, mechanistically, CREB has been implicated in heart failure, and CREB Ser133 phosphorylation enhances the expression of genes related to heart failure (Guo et al., 2010; Chien et al., 2015).

Although activation of AKT initially promotes physiological growth of the heart, constitutive AKT activation leads to pathological cardiac hypertrophy and dysfunction (Chaanine and Hajjar, 2011; Shimizu and Minamino, 2016). In a murine pressure overload model, heterozygous AKT1-deficient ($Akt1^{+/-}$) mice are resistant to pressure overload–induced cardiac dysfunction (Shimizu et al., 2010); however, the mechanism by which this occurs requires further investigation.

Collectively, these data support our findings that Crhr2 antagonism suppresses TAC-induced continuous Gαs/PKA/CREB and Gαs/EPAC/CaMKII pathway activity, thereby attenuating the development of heart failure (Fig. S3 G).

We show in this study that plasma Ucn2 levels significantly increase in patients with heart failure and in mice with pressure overload–induced cardiac dysfunction. Although *Ucn2* mRNA is detected in various tissues, including the brain and heart (Hillhouse and Grammatopoulos, 2006), the secretory organ of Ucn2 remains unclear. In a mouse model of myocardial infarction, Ucn2 expression increases in cardiomyocytes (Li et al., 2013), leading to the hypothesis that cardiomyocytes secrete Ucn2 in heart failure. We measured plasma Ucn2 levels in the peripheral arterial, venous, and coronary sinus blood from patients with NIDCM, but found no significant increase in the coronary sinus sample (unpublished data). Thus, further studies are required to pinpoint the cellular origin of Ucn2 in the context of heart failure.

In conclusion, our data show that Crhr2 activation plays a critical role in the development of heart failure and that Crhr2 antagonist treatment prevents cardiac dysfunction in model mice. Clinical analysis showed significantly elevated plasma Ucn2 in patients with NIDCM compared to healthy subjects. Therefore, Ucn2 may serve as a prognostic indicator for response to Crhr2 inhibitor treatment and facilitate the development of more effective therapies for chronic heart failure.

MATERIALS AND METHODS

Materials and chemicals

Antibodies to Crhr2 (sc-20550), β-actin (sc-47778), Adrb1 (sc-568), Ptger1 (sc-22648), CaMKII (sc-5306), phospho-CaMKII (Thr286, sc-32289), and RyR (sc-376507) were obtained from Santa Cruz Biotechnology, Inc. Antibodies to CREB (48H2, #9197), phospho-CREB (Ser133, 87G3, #9198), PKA (#4782), phospho-PKA (Thr197, #4781), AKT (#9272), and phospho-AKT (Ser473, #4060) were all from Cell Signaling Technology. An antibody to phospho-RyR (Ser2814) was from Badrilla. Human tissue samples were obtained from BioChain.

Western blotting

Cell and tissue samples were lysed in RIPA buffer (Wako) containing a protease inhibitor mixture and phosphatase inhibitor mixture (Roche). Protein concentrations were measured using a BCA protein assay (Thermo Fisher Scientific). Equal amounts of proteins were resolved by SDS-PAGE and transferred onto a PVDF membrane. ECL or ECL plus western blotting detection kits (GE Healthcare) were used for signal detection. Relative phosphorylation and protein levels were quantified with ImageJ software (National Institutes of Health).

Luciferase assay

SNAP antibody (P9310S) and the pSNAPf plasmid were obtained from New England Biolabs. The vectors pGL4.29[luc2P/CRE/Hygro], pGL4.30[luc2P/NFAT-RE/Hygro], pGL4.33[luc2P/SRE/Hygro], and pGL4.34[luc2P/SRF-RE/Hygro] were purchased from Promega. Crhr2 cDNA was from the Kazusa DNA Research Institute. Luciferase reporters for cAMP response element (CRE), nuclear factor of activated T-cells response element (NFAT-RE), serum response element (SRE), and serum response factor response element (SRF-RE, a mutant form of SRE) were used to assess Gs, Gq, Gi, and G12 activation, respectively (Cheng et al., 2010). For luciferase assays, HEK293 cells (JCRB9068, JCRB Cell Bank) were transfected with the indicated plasmids with Lipofectamine 2000 (Invitrogen). Growth medium was replaced with serum-free medium 4 h after transfection, and then cultured for 24 h. Transfected cells were treated with Ucn2 (Peptide Institute) for 24 h and luciferase activities were measured with a luciferase assay system (Promega).

Isolation of adult mouse ventricular cardiomyocytes

Cardiomyocytes were isolated as previously described (Wolska and Solaro, 1996). In brief, mice were heparinized (5,000 IU/kg) and anesthetized with 50 mg/kg sodium pentobarbi-

tal. Hearts were quickly removed, cannulated from the aorta with a blunted 24-gauge needle, and then connected to a perfusion apparatus for retrograde perfusion of the coronary arteries with perfusion buffer (135 mM NaCl, 4.0 mM KCl, 0.33 mM NaH_2PO_4, 1.0 mM $MgCl_2$, 10 mM Hepes, 5 mM taurine, 10 mM 2,3-butanedione monoxime, and 10 mM glucose, pH 7.4) for 3 min (5 ml/min), and then with enzyme buffer, which is the perfusion buffer supplemented with 0.4 mg/ml collagenase D (Roche), 0.5 mg/ml collagenase B (Roche), and 0.06 mg/ml protease XIV (Sigma-Aldrich), for 10 min. After the heart was removed from the perfusion apparatus, atria were removed, ventricles were cut and separated into small pieces gently with forceps, and pipetted several times in perfusion buffer containing 5% BSA. Cells were plated in MEM (Thermo Fisher Scientific) containing 2.0 mM L-glutamine, 10 mM 2,3-butanedione monoxime, 10 µg/ml insulin, 5.5 µg/ml transferrin, 5.0 ng/ml selenium, and 0.1% BSA for 1 h, at which point media was removed and adherent cells were resuspended in BSA-free culture medium until use, generally within 1–2 h.

mRNA expression analysis

To analyze GPCR expression, RNA was extracted from adult mouse cardiomyocytes with an RNeasy Mini kit (QIAGEN) according to the manufacturer's protocol and reverse-transcribed with a QuantiTect Reverse Transcription kit (QIAGEN). Quantification was performed using a LightCycler 480 Probe Master System (Roche) with primers described in Table S1. Genomic DNA from mouse tails was used as a universal standard to calculate gene copy number per ng of RNA (Yun et al., 2006).

For CREB-related genes, quantitative real-time RT-PCR analysis was assessed on a CFX-96 system using SYBR Premix Ex Taq II (Takara Bio), which includes a double-stranded DNA-specific dye, according to the manufacturer's instructions (Bio-Rad Laboratory). PCR primer sequences were as follows: *Agt*, forward 5′-GTTCTCAATAGCATCCTCCT-3′, reverse 5′-CAGGAAGGGGCTGCTCAGG-3′; *Ccr5*, forward 5′-GATTTTCAAGGGTCAGTCC-3′, reverse 5′-GGTATA GACTGAGCTTGCAC-3′; *Foxo3*, forward 5′-CGTAGT GAACTCATGGATGC-3′, reverse 5′-GCTTTGAGATGA GGCCTGCT-3′; *Irs2*, forward 5′-GGGTCCTTGGCGCAG TCTCA-3′, reverse 5′-GCCTGGACCCCCACACACTC-3′; *Ptk2b*, forward 5′-GGGTCCTTGGCGCAGTCTCA-3′, reverse 5′-GACAGGCGGACAGAGAGTTCGG-3′; *Sik1*, forward 5′-CCCTTATTATTCCCCTGGA-3′, reverse 5′-CTC TAGGCTGGGACCCTGCC-3′; *Nr4a1* forward 5′-CGC ACAGTACAGAAAAGCGC-3′, reverse 5′-CTTCACCAT GCCCACAGCCA-3′; and *Gapdh*, forward 5′-TGTGTCCGT CGTGGATCTGA-3′, reverse 5′-TTGCTGTTGAAGTCG CAGGAG-3′. Data are presented after normalization to *Gapdh*.

Tamoxifen-inducible, cardiomyocyte-specific Crhr2 knockout mice (cmc-Crhr2-KO)

$Crhr2^{tm1a(KOMP)Wtsi}$ mice on a C57BL/6 background were generated by the Knock Out Mice Program (KOMP) at the University of California Davis (Davis, CA) and Children's Hospital Oakland Research Institute (Oakland, CA). $Crhr2^{tm1a(KOMP)Wtsi}$ mice were bred with mice expressing Flp recombinase to obtain Crhr2 conditional KO mice ($Crhr2^{flox/flox}$ mice). $Crhr2^{flox/flox}$ mice were backcrossed at least 10 times to wild-type C57BL/6 genetic background mice. Tamoxifen-inducible, cardiomyocyte-specific Crhr2 knockout mice (cmc-Crhr2-KOs) were generated by intercrossing the αMHC–CreERT2 line to $Crhr2^{flox/flox}$ mice (Takefuji et al., 2012). Cre-mediated recombination of floxed alleles was induced with an intraperitoneal injection of 1 mg tamoxifen dissolved in 100 µl Miglyol for 5 consecutive days. Vehicle-treated mice received Miglyol only, and αMHC–$CreERT2^{+/-}$-$Crhr2^{wt/wt}$ mice were used as controls. Experiments were performed 2 wk after the end of induction.

Surgical interventions: osmotic minipumps and transverse aortic constriction

8–10-week-old male mice were anesthetized with 50 mg/kg sodium pentobarbital, and osmotic minipumps (Alzet) containing Ucn2 (100 ng/g/day; Peptide Institute) or antisauvagine-30 (100 ng/g/day; Medical & Biological Laboratories) were implanted subcutaneously in the back for 4 wk.

TAC was performed under anesthesia and intubation. The chest was opened to visualize the aortic arch. The transverse aorta was then ligated between the right innominate and left common carotid arteries against a blunted 24-G needle with a 7–0 suture. The sham procedure was identical except that the aorta was not ligated.

Transthoracic echocardiography was performed on mice anesthetized with 50 mg/kg sodium pentobarbital. The left ventricular (LV) end-systolic diameter and the LV end-diastolic diameters were measured to calculate the %LV fractional shortening (%FS) in M-mode using an Acuson Sequoia C-512 (Siemens) with a 15-MHz probe. SBP was measured by tail cuff method with an automatic sphygmomanometer (BP98A; Saffron) while the mice were restrained.

Mouse plasma Ucn2 and BNP were quantified by a mouse Ucn2 ELISA kit (Yanaihara), and by a BNP Enzyme Immunoassay kit (RayBiotech Inc.), respectively, according to the manufacturer's instructions.

Histological analysis

Tissue samples were embedded in OCT compound (Sakura Finetek) and snap-frozen in liquid nitrogen. Left ventricular myocardium sections (6-µm slices) were stained with Picro-Sirius red with standard protocols and viewed with a BX51 microscope (Olympus). Cardiac fibrosis in 20 random images was quantified in ImageJ software.

Clinical data of human subjects

Blood samples were collected from patients diagnosed with NIDCM at Nagoya University hospital from August 2006 to November 2011. All patients showed stable disease and were hospitalized for detailed cardiac examination by laboratory

analysis, echocardiography, and cardiac catheterization. NID CM was defined as left ventricular ejection fraction (LVEF) <50% on left ventriculography and a dilated LV cavity (LV end-diastolic dimension >55 mm determined by echocardiography), in the absence of coronary heart disease, valvular heart disease, or secondary cardiac muscle disease caused by any known systemic conditions, as determined by endomyocardial biopsy. Of 52 patients, 36 (69.2%) received angiotensin-converting enzyme inhibitors or aldosterone receptor antagonists, 30 (57.7%) received β blockers, and 21 (40.4%) received mineralocorticoid receptor antagonists. Blood samples were collected from the antecubital vein of fasting patients in the morning after resting for 20 min in the supine position. Control blood samples were collected from age- and gender-matched healthy participants of a community-based cohort study without a history of metabolic, cardiovascular, or cancerous diseases. BMI was calculated as follows: BMI = weight (kg)/height $(m)^2$. SBP and diastolic blood pressure (DBP) were measured with a sphygmomanometer, placed on the right arm of each subject with the appropriate cuff size. Plasma total cholesterol, creatinine, and glucose levels were measured by enzymatic methods. BNP (RayBiotech Inc.) and Ucn2 levels (USCN Life Science) were measured by ELISA.

RNA-sequencing

Total RNA was used to generate the cDNA library for subsequent cluster generation using the TruSeq RNA Sample Preparation kit v2 (Illumina). The first step in the workflow involves purifying the poly-A containing mRNA molecules using poly-T oligo-attached magnetic beads. Following purification, the mRNA is fragmented into small pieces under elevated temperature. The cleaved RNA fragments are then used for first strand cDNA synthesis with reverse transcriptase and random primers, followed by second strand cDNA synthesis. These cDNA fragments then go through an end repair process, the addition of a single "A" base, and ligation of the adapters. The products are then purified and enriched with PCR to create the final cDNA library. The libraries were sequenced on an Illumina HiSeq2500 platform in a paired-end 100-bp configuration.

Adapter and low-quality sequences were removed by cutadapt (v1.2.1). After quality control analysis, poly-A/T sequences were removed by PRINSEQ (v0.19.2; Schmieder and Edwards, 2011). To determine gene expression, trimmed reads were aligned to the reference human genome (GRCh37/hg19) using TopHat (v2.0.13; Trapnell et al., 2009). Mapped reads were assembled by Cufflinks (v2.2.1; Trapnell et al., 2010), and the transcripts across all samples were merged with Cuffmerge, which is part of the Cufflinks package. The fragments per kilo base per million mapped reads (FPKM) was calculated with Cuffquant, and differential expression analysis between samples was performed with Cuffdiff.

To identify candidates from the total gene pool (28,522 genes), we set the t-value cut-off at <0.01 (255 genes), and FPKM at a >1.5-fold increase compared to controls (88 genes). We then queried genes related to: CREB (29 genes), MEF2 (8 genes), or heart failure (15 genes), the CREB response element; genes harboring TGACGTCA, TGACG, or CGTCA sequences (Altarejos and Montminy, 2011); or MEF2 response elements; genes harboring a $CTA(A/T)_4TAG/A$ sequence (Akazawa and Komuro, 2003) within 3,000-bp upstream to 300-bp downstream of the transcription start site; heart failure–related genes, genes previously associated with heart failure. Six genes related to both CREB and heart failure, and one gene (*Nr4a1*), which was related to CREB, MEF2, and heart failure, were identified as target genes.

Study approval

The clinical study protocol was approved by the Ethics Review Board of Nagoya University School of Medicine and Jichi Medical University. Written informed consent was obtained from all study subjects. All procedures of animal care and animal use in this study were approved by the Animal Ethics Review Board of Nagoya University School of Medicine.

Statistical analysis

Data are presented as the means ± SEM in animal experiments and the means ± SD, medians (interquartile ranges), or subject numbers (%) in human subjects. All statistical analyses for animal experiments were performed in GraphPad Prism 6. Comparisons between two groups were performed with unpaired Student's t or Chi-square tests, while those between more than two groups were done using ANOVA with Bonferroni post-hoc testing. Survival curves were analyzed with Kaplan Meyer estimators and Log-rank (Mantel-Cox) testing. Comparisons between more than two groups at different time points were performed by two-way ANOVA, followed by Bonferroni post-hoc test.

Since Ucn2 showed a skewed distribution in the human studies, the variables were log-transformed before analysis, and differences were assessed using a general linear model with parameter adjustments. Significance was defined as $P < 0.05$ (*, $P < 0.05$; **, $P < 0.01$).

Online supplemental material

Fig. S1 shows a flow chart of GPCR screening. Fig. S2 shows that Ucn2 caused further cardiac dysfunction induced by pressure overload. Fig. S3 shows Ucn2-mediated cellular signaling in the heart. Table S1 shows probes and primer sequences for quantification of mouse GPCR expression.

ACKNOWLEDGMENTS

We thank the staff from the Division of Experimental Animals, Nagoya University School of Medicine for assisting with animal experiments.

This work was supported by a Grant-in-Aid for Scientific Research (C) from the Ministry of Education, Culture, Sports, Science and Technology of Japan (to M. Takefuji) and by the Takeda Science Foundation (to M. Takefuji).

The authors declare no competing financial interests.

Author contributions: M. Takefuji, N. Wettschureck, and S. Offermans. designed the experiments. T. Tsuda, H. Kaur, S. Eguchi, T. Sakaguchi, and S. Ishihama performed the animal experiments. K. Kotani, R. Morimoto, T. Okumura, and S. Ishikawa collected human samples and were responsible for obtaining clinical information. R. Kikuchi examined human samples. T. Tsuda and M. Takefuji wrote the manuscript, with contributions from N. Wettschureck, K. Kotani, K. Unno, K. Matsushita, S. Offermanns, and T. Murohara.

Submitted: 17 November 2016

Revised: 9 March 2017

Accepted: 12 April 2017

REFERENCES

Adão, R., D. Santos-Ribeiro, M.T. Rademaker, A.F. Leite-Moreira, and C. Brás-Silva. 2015. Urocortin 2 in cardiovascular health and disease. *Drug Discov. Today.* 20:906–914. http://dx.doi.org/10.1016/j.drudis.2015.02.012

Akazawa, H., and I. Komuro. 2003. Roles of cardiac transcription factors in cardiac hypertrophy. *Circ. Res.* 92:1079–1088. http://dx.doi.org/10.1161/01.RES.0000072977.86706.23

Altarejos, J.Y., and M. Montminy. 2011. CREB and the CRTC co-activators: sensors for hormonal and metabolic signals. *Nat. Rev. Mol. Cell Biol.* 12:141–151. http://dx.doi.org/10.1038/nrm3072

Anderson, M.E., J.H. Brown, and D.M. Bers. 2011. CaMKII in myocardial hypertrophy and heart failure. *J. Mol. Cell. Cardiol.* 51:468–473. http://dx.doi.org/10.1016/j.yjmcc.2011.01.012

Antos, C.L., N. Frey, S.O. Marx, S. Reiken, M. Gaburjakova, J.A. Richardson, A.R. Marks, and E.N. Olson. 2001. Dilated cardiomyopathy and sudden death resulting from constitutive activation of protein kinase a. *Circ. Res.* 89:997–1004. http://dx.doi.org/10.1161/hh2301.100003

Backs, J., and E.N. Olson. 2006. Control of cardiac growth by histone acetylation/deacetylation. *Circ. Res.* 98:15–24. http://dx.doi.org/10.1161/01.RES.0000197782.21444.8f

Bale, T.L., and W.W. Vale. 2004. CRF and CRF receptors: role in stress responsivity and other behaviors. *Annu. Rev. Pharmacol. Toxicol.* 44:525–557. http://dx.doi.org/10.1146/annurev.pharmtox.44.101802.121410

Banerjee, A., V. Pirrone, B. Wigdahl, and M.R. Nonnemacher. 2011. Transcriptional regulation of the chemokine co-receptor CCR5 by the cAMP/PKA/CREB pathway. *Biomed. Pharmacother.* 65:293–297. http://dx.doi.org/10.1016/j.biopha.2011.03.009

Berdeaux, R., N. Goebel, L. Banaszynski, H. Takemori, T. Wandless, G.D. Shelton, and M. Montminy. 2007. SIK1 is a class II HDAC kinase that promotes survival of skeletal myocytes. *Nat. Med.* 13:597–603. http://dx.doi.org/10.1038/nm1573

Boularan, C., and C. Gales. 2015. Cardiac cAMP: production, hydrolysis, modulation and detection. *Front. Pharmacol.* 6:203. http://dx.doi.org/10.3389/fphar.2015.00203

Braunwald, E. 2001. Expanding indications for beta-blockers in heart failure. *N. Engl. J. Med.* 344:1711–1712. http://dx.doi.org/10.1056/NEJM200105313442210

Braunwald, E. 2013. Heart failure. *JACC Heart Fail.* 1:1–20. http://dx.doi.org/10.1016/j.jchf.2012.10.002

Capote, L.A., R. Mendez Perez, and A. Lymperopoulos. 2015. GPCR signaling and cardiac function. *Eur. J. Pharmacol.* 763(Pt B):143–148. http://dx.doi.org/10.1016/j.ejphar.2015.05.019

Chaanine, A.H., and R.J. Hajjar. 2011. AKT signalling in the failing heart. *Eur. J. Heart Fail.* 13:825–829. http://dx.doi.org/10.1093/eurjhf/hfr080

Chan, W.Y., C.M. Frampton, I.G. Crozier, R.W. Troughton, and A.M. Richards. 2013. Urocortin-2 infusion in acute decompensated heart failure: findings from the UNICORN study (urocortin-2 in the treatment of acute heart failure as an adjunct over conventional therapy). *JACC Heart Fail.* 1:433–441. http://dx.doi.org/10.1016/j.jchf.2013.07.003

Chen, A., M. Perrin, B. Brar, C. Li, P. Jamieson, M. Digruccio, K. Lewis, and W. Vale. 2005. Mouse corticotropin-releasing factor receptor type 2alpha gene: isolation, distribution, pharmacological characterization and regulation by stress and glucocorticoids. *Mol. Endocrinol.* 19:441–458. http://dx.doi.org/10.1210/me.2004-0300

Cheng, Z., D. Garvin, A. Paguio, P. Stecha, K. Wood, and F. Fan. 2010. Luciferase Reporter Assay System for Deciphering GPCR Pathways. *Curr. Chem. Genomics.* 4:84–91. http://dx.doi.org/10.2174/1875397301004010084

Chien, P.T., C.C. Lin, L.D. Hsiao, and C.M. Yang. 2015. c-Src/Pyk2/EGFR/PI3K/Akt/CREB-activated pathway contributes to human cardiomyocyte hypertrophy: Role of COX-2 induction. *Mol. Cell. Endocrinol.* 409:59–72. http://dx.doi.org/10.1016/j.mce.2015.04.005

Cong, B., Y. Xu, H. Sheng, X. Zhu, L. Wang, W. Zhao, Z. Tang, J. Lu, and X. Ni. 2014. Cardioprotection of 17β-estradiol against hypoxia/reoxygenation in cardiomyocytes is partly through up-regulation of CRH receptor type 2. *Mol. Cell. Endocrinol.* 382:17–25. http://dx.doi.org/10.1016/j.mce.2013.09.002

Coste, S.C., R.A. Kesterson, K.A. Heldwein, S.L. Stevens, A.D. Heard, J.H. Hollis, S.E. Murray, J.K. Hill, G.A. Pantely, A.R. Hohimer, et al. 2000. Abnormal adaptations to stress and impaired cardiovascular function in mice lacking corticotropin-releasing hormone receptor-2. *Nat. Genet.* 24:403–409. http://dx.doi.org/10.1038/74255

Davis, M.E., C.J. Pemberton, T.G. Yandle, S.F. Fisher, J.G. Lainchbury, C.M. Frampton, M.T. Rademaker, and A.M. Richards. 2007a. Urocortin 2 infusion in healthy humans: hemodynamic, neurohormonal, and renal responses. *J. Am. Coll. Cardiol.* 49:461–471. http://dx.doi.org/10.1016/j.jacc.2006.09.035

Davis, M.E., C.J. Pemberton, T.G. Yandle, S.F. Fisher, J.G. Lainchbury, C.M. Frampton, M.T. Rademaker, and M. Richards. 2007b. Urocortin 2 infusion in human heart failure. *Eur. Heart J.* 28:2589–2597. http://dx.doi.org/10.1093/eurheartj/ehm340

Doust, J.A., E. Pietrzak, A. Dobson, and P. Glasziou. 2005. How well does B-type natriuretic peptide predict death and cardiac events in patients with heart failure: systematic review. *BMJ.* 330:625. http://dx.doi.org/10.1136/bmj.330.7492.625

Engelhardt, S., L. Hein, F. Wiesmann, and M.J. Lohse. 1999. Progressive hypertrophy and heart failure in beta1-adrenergic receptor transgenic mice. *Proc. Natl. Acad. Sci. USA.* 96:7059–7064. http://dx.doi.org/10.1073/pnas.96.12.7059

Engelman, J.A., J. Luo, and L.C. Cantley. 2006. The evolution of phosphatidylinositol 3-kinases as regulators of growth and metabolism. *Nat. Rev. Genet.* 7:606–619. http://dx.doi.org/10.1038/nrg1879

Fang, J., G.A. Mensah, J.B. Croft, and N.L. Keenan. 2008. Heart failure-related hospitalization in the U.S., 1979 to 2004. *J. Am. Coll. Cardiol.* 52:428–434. http://dx.doi.org/10.1016/j.jacc.2008.03.061

Fentzke, R.C., C.E. Korcarz, R.M. Lang, H. Lin, and J.M. Leiden. 1998. Dilated cardiomyopathy in transgenic mice expressing a dominant-negative CREB transcription factor in the heart. *J. Clin. Invest.* 101:2415–2426. http://dx.doi.org/10.1172/JCI2950

Frey, N., and E.N. Olson. 2003. Cardiac hypertrophy: the good, the bad, and the ugly. *Annu. Rev. Physiol.* 65:45–79. http://dx.doi.org/10.1146/annurev.physiol.65.092101.142243

Gao, M.H., N.C. Lai, A. Miyanohara, J.M. Schilling, J. Suarez, T. Tang, T. Guo, R. Tang, J. Parikh, D. Giamouridis, et al. 2013. Intravenous adeno-associated virus serotype 8 encoding urocortin-2 provides sustained augmentation of left ventricular function in mice. *Hum. Gene Ther.* 24:777–785. http://dx.doi.org/10.1089/hum.2013.088

Geng, Y.J., Y. Ishikawa, D.E. Vatner, T.E. Wagner, S.P. Bishop, S.F. Vatner, and C.J. Homcy. 1999. Apoptosis of cardiac myocytes in Gsalpha transgenic mice. *Circ. Res.* 84:34–42. http://dx.doi.org/10.1161/01.RES.84.1.34

Guo, D., Z. Kassiri, R. Basu, F.L. Chow, V. Kandalam, F. Damilano, W. Liang, S. Izumo, E. Hirsch, J.M. Penninger, et al. 2010. Loss of PI3Kγ enhances cAMP-dependent MMP remodeling of the myocardial N-cadherin adhesion complexes and extracellular matrix in response to early biomechanical stress. *Circ. Res.* 107:1275–1289. http://dx.doi.org/10.1161/CIRCRESAHA.110.229054

Heineke, J., and J.D. Molkentin. 2006. Regulation of cardiac hypertrophy by intracellular signalling pathways. *Nat. Rev. Mol. Cell Biol.* 7:589–600. http://dx.doi.org/10.1038/nrm1983

Heng, B.C., D. Aubel, and M. Fussenegger. 2013. An overview of the diverse roles of G-protein coupled receptors (GPCRs) in the pathophysiology of various human diseases. *Biotechnol. Adv.* 31:1676–1694. http://dx.doi.org/10.1016/j.biotechadv.2013.08.017

Hill, J.A., and E.N. Olson. 2008. Cardiac plasticity. *N. Engl. J. Med.* 358:1370–1380. http://dx.doi.org/10.1056/NEJMra072139

Hillhouse, E.W., and D.K. Grammatopoulos. 2006. The molecular mechanisms underlying the regulation of the biological activity of corticotropin-releasing hormone receptors: implications for physiology and pathophysiology. *Endocr. Rev.* 27:260–286. http://dx.doi.org/10.1210/er.2005-0034

Iwase, M., S.P. Bishop, M. Uechi, D.E. Vatner, R.P. Shannon, R.K. Kudej, D.C. Wight, T.E. Wagner, Y. Ishikawa, C.J. Homcy, and S.F. Vatner. 1996. Adverse effects of chronic endogenous sympathetic drive induced by cardiac GS alpha overexpression. *Circ. Res.* 78:517–524. http://dx.doi.org/10.1161/01.RES.78.4.517

Jessup, M., and S. Brozena. 2003. Heart failure. *N. Engl. J. Med.* 348:2007–2018. http://dx.doi.org/10.1056/NEJMra021498

Jhala, U.S., G. Canettieri, R.A. Screaton, R.N. Kulkarni, S. Krajewski, J. Reed, J. Walker, X. Lin, M. White, and M. Montminy. 2003. cAMP promotes pancreatic beta-cell survival via CREB-mediated induction of IRS2. *Genes Dev.* 17:1575–1580. http://dx.doi.org/10.1101/gad.1097103

Kang, M., K.Y. Chung, and J.W. Walker. 2007. G-protein coupled receptor signaling in myocardium: not for the faint of heart. *Physiology (Bethesda).* 22:174–184. http://dx.doi.org/10.1152/physiol.00051.2006

Katritch, V., V. Cherezov, and R.C. Stevens. 2013. Structure-function of the G protein-coupled receptor superfamily. *Annu. Rev. Pharmacol. Toxicol.* 53:531–556. http://dx.doi.org/10.1146/annurev-pharmtox-032112-135923

Kishimoto, T., R.V. Pearse II, C.R. Lin, and M.G. Rosenfeld. 1995. A sauvagine/corticotropin-releasing factor receptor expressed in heart and skeletal muscle. *Proc. Natl. Acad. Sci. USA.* 92:1108–1112. http://dx.doi.org/10.1073/pnas.92.4.1108

Lezoualc'h, F., L. Fazal, M. Laudette, and C. Conte. 2016. Cyclic AMP sensor EPAC proteins and their role in cardiovascular function and disease. *Circ. Res.* 118:881–897. http://dx.doi.org/10.1161/CIRCRESAHA.115.306529

Li, J., D. Qi, H. Cheng, X. Hu, E.J. Miller, X. Wu, K.S. Russell, N. Mikush, J. Zhang, L. Xiao, et al. 2013. Urocortin 2 autocrine/paracrine and pharmacologic effects to activate AMP-activated protein kinase in the heart. *Proc. Natl. Acad. Sci. USA.* 110:16133–16138. http://dx.doi.org/10.1073/pnas.1312775110

Lymperopoulos, A., G. Rengo, and W.J. Koch. 2013. Adrenergic nervous system in heart failure: pathophysiology and therapy. *Circ. Res.* 113:739–753. http://dx.doi.org/10.1161/CIRCRESAHA.113.300308

Marx, S.O., S. Reiken, Y. Hisamatsu, T. Jayaraman, D. Burkhoff, N. Rosemblit, and A.R. Marks. 2000. PKA phosphorylation dissociates FKBP12.6 from the calcium release channel (ryanodine receptor): defective regulation in failing hearts. *Cell.* 101:365–376. http://dx.doi.org/10.1016/S0092-8674(00)80847-8

Matus, M., G. Lewin, F. Stümpel, I.B. Buchwalow, M.D. Schneider, G. Schütz, W. Schmitz, and F.U. Müller. 2007. Cardiomyocyte-specific inactivation of transcription factor CREB in mice. *FASEB J.* 21:1884–1892. http://dx.doi.org/10.1096/fj.06-7915com

Mayr, B., and M. Montminy. 2001. Transcriptional regulation by the phosphorylation-dependent factor CREB. *Nat. Rev. Mol. Cell Biol.* 2:599–609. http://dx.doi.org/10.1038/35085068

Overington, J.P., B. Al-Lazikani, and A.L. Hopkins. 2006. How many drug targets are there? *Nat. Rev. Drug Discov.* 5:993–996. http://dx.doi.org/10.1038/nrd2199

Regard, J.B., I.T. Sato, and S.R. Coughlin. 2008. Anatomical profiling of G protein-coupled receptor expression. *Cell.* 135:561–571. http://dx.doi.org/10.1016/j.cell.2008.08.040

Rühmann, A., I. Bonk, C.R. Lin, M.G. Rosenfeld, and J. Spiess. 1998. Structural requirements for peptidic antagonists of the corticotropin-releasing factor receptor (CRFR): development of CRFR2beta-selective antisauvagine-30. *Proc. Natl. Acad. Sci. USA.* 95:15264–15269. http://dx.doi.org/10.1073/pnas.95.26.15264

Salazar, N.C., J. Chen, and H.A. Rockman. 2007. Cardiac GPCRs: GPCR signaling in healthy and failing hearts. *Biochim. Biophys. Acta.* 1768:1006–1018. http://dx.doi.org/10.1016/j.bbamem.2007.02.010

Schmieder, R., and R. Edwards. 2011. Quality control and preprocessing of metagenomic datasets. *Bioinformatics.* 27:863–864. http://dx.doi.org/10.1093/bioinformatics/btr026

Shimizu, I., and T. Minamino. 2016. Physiological and pathological cardiac hypertrophy. *J. Mol. Cell. Cardiol.* 97:245–262. http://dx.doi.org/10.1016/j.yjmcc.2016.06.001

Shimizu, H., S. Saito, Y. Higashiyama, F. Nishijima, and T. Niwa. 2013. CREB, NF-κB, and NADPH oxidase coordinately upregulate indoxyl sulfate-induced angiotensinogen expression in proximal tubular cells. *Am. J. Physiol. Cell Physiol.* 304:C685–C692. http://dx.doi.org/10.1152/ajpcell.00236.2012

Shimizu, I., T. Minamino, H. Toko, S. Okada, H. Ikeda, N. Yasuda, K. Tateno, J. Moriya, M. Yokoyama, A. Nojima, et al. 2010. Excessive cardiac insulin signaling exacerbates systolic dysfunction induced by pressure overload in rodents. *J. Clin. Invest.* 120:1506–1514. http://dx.doi.org/10.1172/JCI40096

Steinberg, R.A., R.D. Cauthron, M.M. Symcox, and H. Shuntoh. 1993. Autoactivation of catalytic (C alpha) subunit of cyclic AMP-dependent protein kinase by phosphorylation of threonine 197. *Mol. Cell. Biol.* 13:2332–2341. http://dx.doi.org/10.1128/MCB.13.4.2332

Stenzel, P., R. Kesterson, W. Yeung, R.D. Cone, M.B. Rittenberg, and M.P. Stenzel-Poore. 1995. Identification of a novel murine receptor for corticotropin-releasing hormone expressed in the heart. *Mol. Endocrinol.* 9:637–645.

Takefuji, M., A. Wirth, M. Lukasova, S. Takefuji, T. Boettger, T. Braun, T. Althoff, S. Offermanns, and N. Wettschureck. 2012. G(13)-mediated signaling pathway is required for pressure overload-induced cardiac remodeling and heart failure. *Circulation.* 126:1972–1982. http://dx.doi.org/10.1161/CIRCULATIONAHA.112.109256

Tamargo, J., and J. López-Sendón. 2011. Novel therapeutic targets for the treatment of heart failure. *Nat. Rev. Drug Discov.* 10:536–555. http://dx.doi.org/10.1038/nrd3431

Trapnell, C., L. Pachter, and S.L. Salzberg. 2009. TopHat: discovering splice junctions with RNA-Seq. *Bioinformatics.* 25:1105–1111. http://dx.doi.org/10.1093/bioinformatics/btp120

Trapnell, C., B.A. Williams, G. Pertea, A. Mortazavi, G. Kwan, M.J. van Baren, S.L. Salzberg, B.J. Wold, and L. Pachter. 2010. Transcript assembly and quantification by RNA-Seq reveals unannotated transcripts and isoform

switching during cell differentiation. *Nat. Biotechnol.* 28:511–515. http://dx.doi.org/10.1038/nbt.1621

Wettschureck, N., and S. Offermanns. 2005. Mammalian G proteins and their cell type specific functions. *Physiol. Rev.* 85:1159–1204. http://dx.doi.org/10.1152/physrev.00003.2005

Wolska, B.M., and R.J. Solaro. 1996. Method for isolation of adult mouse cardiac myocytes for studies of contraction and microfluorimetry. *Am. J. Physiol.* 271:H1250–H1255.

Yancy, C.W., M. Jessup, B. Bozkurt, J. Butler, D.E. Casey Jr., M.H. Drazner, G.C. Fonarow, S.A. Geraci, T. Horwich, J.L. Januzzi, et al. American College of Cardiology Foundation/American Heart Association Task Force on Practice Guidelines. 2013. 2013 ACCF/AHA guideline for the management of heart failure: a report of the American College of Cardiology Foundation/American Heart Association Task Force on practice guidelines. *Circulation.* 128:e240–e327. http://dx.doi.org/10.1161/CIR.0b013e31829e8807

Yun, J.J., L.E. Heisler, I.I. Hwang, O. Wilkins, S.K. Lau, M. Hyrcza, B. Jayabalasingham, J. Jin, J. McLaurin, M.S. Tsao, and S.D. Der. 2006. Genomic DNA functions as a universal external standard in quantitative real-time PCR. *Nucleic Acids Res.* 34:e85. http://dx.doi.org/10.1093/nar/gkl400